CIRP Journal of Manufacturing Science and Technology 1 (2008) 35–44

Contents lists available at ScienceDirect

CIRP Journal of Manufacturing Science and Technology

journal homepage: www.elsevier.com/locate/cirpj

Chatter stability of milling in frequency and discrete time domain

Y. Altintas [a,*], G. Stepan [b], D. Merdol [a], Z. Dombovari [b]

[a] Manufacturing Automation Laboratory, Department of Mechanical Engineering, The University of British Columbia, 2054-6250 Applied Science Lane, Vancouver, B.C. V6T 1Z4, Canada[1]

[b] Department of Applied Mechanics, Budapest University of Technology and Economics, Muegyetem rkp. 5., 1111 Budapest, Hungary[2]

ARTICLE INFO

Article history:
Available online 10 July 2008

Keywords:
Chatter
Milling
Stability

ABSTRACT

Chatter stability of milling operations has been gaining significant attention with a view to improving the material removal rates in high speed machining of aluminum alloys and low speed milling of difficult to cut, thermal resistant alloys. This paper presents frequency and discrete time domain chatter stability laws for milling operations in a unified manner. The time periodic dynamics of the milling process are modelled. By averaging time varying directional factors at cutter pitch intervals, the stability lobes are solved directly and analytically. When the process is highly intermittent, which occurs at high speeds and low radial depth of cuts, the stability lobes are more accurately solved either by taking higher harmonics of directional factors in frequency domain, or by using semi-discretization method. This paper compares the stability solutions against the numerical solutions and experiments, and provides comprehensive mathematical details of both fundamental stability solutions.

1. Introduction

Chatter is a form of self-excited, unstable vibration during metal cutting. When the cutting force creates a relative displacement between flexible tool and work-piece at the cutting point, the chip thickness experiences waves on its inner and outer surfaces due to present and past vibrations. The dynamics of the cutting system are defined by coupled, delayed differential equations. Depending on the gain of the system and the phase between the inner and outer waves, the dynamics of the cutting system can be unstable, leading to exponentially growing chips, hence large forces and vibrations until the tool jumps out of the cut or machine tool set up is damaged. It has been the objective of researchers to model the dynamics of the metal cutting system and predict relationships between work material, structural dynamics of the machine, tool geometry and cutting conditions. The mathematical model of the stability leads to better machine tool and cutting tool design, as well as prediction of the most productive cutting conditions ahead of costly machining trials.

Koenigsberger and Tlusty [1] and Tobias [2] were the leading pioneers in formulating the mechanisms behind the chip regeneration and one-dimensional chatter stability formulation. They assumed that the direction of the cutting force as well as the projected vibrations along the chip thickness are constant, which is true for single point cutting operations like turning, boring and broaching. Tlusty presented a simple relationship between the maximum depth of cut, stiffness of the structure and specific cutting coefficient of the process. His equation gives the maximum depth of cut as being linearly proportional to dynamic stiffness and inversely proportional to the cutting coefficient. Higher dynamic stiffness and a lower material cutting coefficient (i.e. hardness) lead to high material removal rates. Tobias proposed a similar model, but included the influence of the phase between the inner and outer waves left on the chip surface, and invented stability lobes [2]. The stability lobes led to the high material removal rates in milling aluminum alloys at high spindle speeds [3].

Unlike single point metal cutting, milling is conducted with a rotating cutter having multiple teeth. The directions of the forces vary as the cutter rotates, and the system is periodic at tooth passing intervals when the cutter has a uniform pitch or at spindle intervals if the tooth spacing is variable. Tlusty and co-workers presented the numerical simulation of the milling dynamics including saturations such as the tool jumping out of cut [4,5]. The closed form dynamic of the milling system was formulated by

* Corresponding author.
E-mail addresses: altintas@interchange.ubc.ca (Y. Altintas), stepan@mm.bme.hu (G. Stepan).
[1] http://www.mech.ubc.ca/~mal.
[2] http://www.mm.bme.hu.

1755-5817/$ – see front matter © 2008 CIRP.
doi:10.1016/j.cirpj.2008.06.003

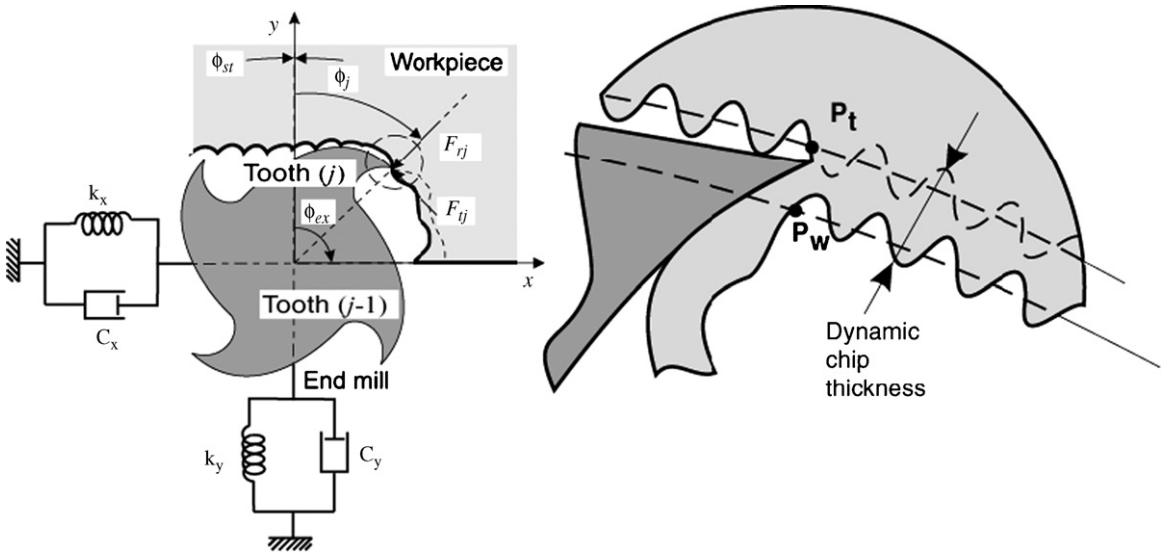

Fig. 1. Dynamic milling system.

Sridhar et al. [6], but its analytical solution was first successfully accomplished by Minis et al. [7], who used Floquet theory to assess the stability for given cutting conditions. Altintas and Budak [8] presented the first analytical solution that led to the prediction of stability lobes directly in the frequency domain. Budak and Altintas [9] also demonstrate a higher order solution which provides improved prediction when the process is highly intermittent at small radial immersions. Stépán and co-workers [10–12] and Bayly et al. [13] solved the stability in discrete time domain, which allowed for inclusion of periodically varying system parameters directly. The remaining research efforts mainly extended application of the frequency and discrete time domain solutions presented in this paper.

This paper presents frequency and semi-discrete time domain solutions of the chatter stability proposed by the authors. The zero order and multi-frequency solutions of milling stability presented by Altintas and Budak [8] and Budak and Altintas [9] are summarized. A semi-discrete time domain solution of the milling stability of Stépán and co-workers [10–12] is also presented. A comparison of the two models and their advantages at different cutting conditions is presented with simple examples. The paper is concluded with a summary of the applications of each technique. It is hoped that the paper provides a comprehensive theoretical insight into the milling chatter stability to metal cutting researchers.

2. Dynamics of milling

A milling cutter with N teeth is considered to have flexibility in two orthogonal directions (x,y) as shown in Fig. 1. The vibrations are projected to rotating tooth number j in the radial or chip thickness direction at instantaneous angular immersion ϕ_j of tooth j measured clockwise from the normal (y) axis. If the spindle rotates at an angular speed of Ω (rad/s), the resulting regenerative, dynamic chip thickness caused by vibrations is [8]

$$h_j(t) = (\Delta x(t)\sin\phi_j(t) + \Delta y(t)\cos\phi_j(t))g(\phi_j(t)), \tag{1}$$

where the differenced vibrations are $\Delta x(t) = x(t) - x(t-T)$, $\Delta y(t) = y(t) - y(t-T)$, and T is the tooth passing interval. The function $g(\phi_j)$ is used to indicate whether the tooth is in or out of the cut

$$g(\phi_j) = \begin{cases} 1, & \text{if} \quad \phi_{st} < \phi_j < \phi_{ex}, \\ 0, & \text{otherwise}, \end{cases} \tag{2}$$

where ϕ_{st} and ϕ_{ex} are the start and exit immersion angles of the cutter to and from the cut, respectively. The tangential (F_{tj}) and radial (F_{rj}) cutting forces acting on the tooth j are proportional to the axial depth of the cut (a) and chip thickness (h):

$$F_{tj}(t) = K_t a\, h_j(t), \qquad F_{rj}(t) = K_r F_{tj}(t), \tag{3}$$

where cutting coefficients K_t and K_r are constant. Resolving the cutting forces in the x and y directions

$$\begin{aligned} F_{xj} &= -F_{tj}\cos\phi_j - F_{rj}\sin\phi_j, \\ F_{yj} &= +F_{tj}\sin\phi_j - F_{rj}\cos\phi_j, \end{aligned} \tag{4}$$

and summing the cutting forces contributed by all teeth, the total dynamic milling forces acting on the cutter become

$$F_x = \sum_{j=0}^{N-1} F_{xj}, \qquad F_y = \sum_{j=0}^{N-1} F_{yj}, \tag{5}$$

where $\phi_j = \phi + j\phi_p$ and cutter pitch angle is $\phi_p = 2\pi/N$. Substituting the chip thickness (1) and tooth forces (3) into (4) and rearranging the resulting expressions in matrix form yields

$$\begin{Bmatrix} F_x \\ F_y \end{Bmatrix} = \frac{1}{2} a K_t \begin{bmatrix} a_{xx} & a_{xy} \\ a_{yx} & a_{yy} \end{bmatrix} \begin{Bmatrix} \Delta x \\ \Delta y \end{Bmatrix}, \tag{6}$$

where time-varying directional dynamic milling force coefficients are given by

$$[A(t)] = \begin{bmatrix} a_{xx}(t) & a_{xy}(t) \\ a_{yx}(t) & a_{yy}(t) \end{bmatrix} = \begin{bmatrix} \sum_{j=0}^{N-1} -g_j(t)[\sin 2\phi_j(t) + K_r(1-\cos 2\phi_j(t))] & \sum_{j=0}^{N-1} -g_j(t)[(1+\cos 2\phi_j(t)) + K_r \sin 2\phi_j(t)] \\ \sum_{j=0}^{N-1} g_j(t)[(1-\cos 2\phi_j(t)) - K_r \sin 2\phi_j(t)] & \sum_{j=0}^{N-1} g_j(t)[\sin 2\phi_j(t) - K_r(1+\cos 2\phi_j(t))] \end{bmatrix}. \tag{7}$$

Considering that the angular position of the cutter changes with time and angular velocity, we can express (6) in a matrix form as

$$\{F(t)\} = \frac{1}{2} a K_t [A(t)] \{\Delta(t)\}, \tag{8}$$

where $\{\Delta(t)\} = [\Delta x(t) \quad \Delta y(t)]^T$. As the cutter rotates, the directional factors vary with time, and $[A(t)]$ is periodic at tooth passing frequency $\omega_T = N\Omega$ or tooth period $T = 2\pi/\omega_T$. For the purposes of mathematical illustration, assume that the machine has the following two orthogonal frequency response functions (FRFs) reflected at the cutter

$$\left.\begin{aligned} \Phi_{xx}(\omega) &= \frac{\omega_{nx}^2/k_x}{\omega_{nx}^2 - \omega^2 + i2\varsigma_x\omega_{nx}\omega} \rightarrow \ddot{x}(t) + 2\varsigma_x\omega_{nx}\dot{x}(t) + \omega_{nx}^2 x(t) = \frac{\omega_{nx}^2}{k_x F_x(t)} \\ \Phi_{yy}(\omega) &= \frac{\omega_{ny}^2/k_y}{\omega_{ny}^2 - \omega^2 + i2\varsigma_y\omega_{ny}\omega} \rightarrow \ddot{y}(t) + 2\varsigma_x\omega_{nx}\dot{y}(t) + \omega_{nx}^2 y(t) = \frac{\omega_{ny}^2}{k_y F_y(t)} \end{aligned}\right\}. \tag{9}$$

The structural dynamics of the work-piece can be added to the FRF. The resulting dynamics of the milling process are expressed by the following coupled, delayed differential equations:

$$\begin{Bmatrix} \ddot{x}(t) + 2\varsigma_x\omega_{nx}\dot{x}(t) + \omega_{nx}^2 x(t) \\ \ddot{y}(t) + 2\varsigma_x\omega_{nx}\dot{y}(t) + \omega_{nx}^2 y(t) \end{Bmatrix} = \frac{1}{2} a K_t \begin{bmatrix} \frac{\omega_{nx}^2}{k_x} & 0 \\ 0 & \frac{\omega_{ny}^2}{k_y} \end{bmatrix} \begin{bmatrix} a_{xx}(t) & a_{xy}(t) \\ a_{yx}(t) & a_{yy}(t) \end{bmatrix} \begin{Bmatrix} x(t) - x(t-T) \\ y(t) - y(t-T) \end{Bmatrix}. \tag{10}$$

The chatter stability problem is defined by the prediction of critical axial depth of cut (a) and the tooth period or delay term (T). The delay terms bring both coupling and complexity to the solution of the differential equations. The stability of the system has been solved by Budak and Altintas in frequency domain [8,9] and Insperger and Stépán [10,11], in discrete time domain as summarized below.

3. Frequency domain solution of chatter stability in milling

Altintas and Budak [8] and Budak and Altintas [9] presented the following frequency domain solution for the milling stability problem. If the dynamic milling system is critically stable at a frequency ω, the vibrations $\{Q(\omega)\} = \{x(\omega) \quad y(\omega)\}^T$ are expressed as

$$\{Q(\omega)\} = [\Phi(\omega)]\{F(\omega)\}. \tag{11}$$

The dynamic force is converted from time (8) to frequency domain:

$$\{F(\omega)\} = \frac{1}{2} a K_t \{A(\omega)\} * \{\Delta(\omega)\}, \tag{12}$$

where the * denotes the convolution integral. The differenced vibrations $\{\Delta(\omega)\}$ have the following form in frequency domain according to (11):

$$\{\Delta(\omega)\} = (1 - e^{-i\omega T})[\Phi(\omega)]\{F(\omega)\}.$$

Substituting $\{\Delta(\omega)\}$ into the dynamic milling equation gives

$$\{F(\omega)\} = \frac{1}{2} a K_t [A(\omega)] * ((1 - e^{-i\omega T})[\Phi(\omega)]\{F(\omega)\}). \tag{13}$$

The periodic directional matrix can be expanded into a *Fourier series*:

$$\left.\begin{aligned} [A(\omega)] &= \sum_{r=-\infty}^{\infty} [A_r]\delta(\omega - r\omega_T) = \mathcal{F}[A(t)] = \left(\sum_{r=-\infty}^{\infty} [A_r] e^{ir\omega_T t}\right) \\ [A_r] &= \frac{1}{T}\int_0^T [A(t)] e^{-ir\omega_T t} dt \end{aligned}\right\} \tag{14}$$

where δ and $\mathcal{F}$ denote the *Dirac delta* function and the *Fourier transformation*, respectively. The directional matrix $[A(t)]$ is periodic at tooth passing frequency ω_T or at cutter pitch angle ϕ_p, and it has zero value when the tooth is out of cut, i.e. $\phi_{st} \le \phi \le \phi_{ex} \rightarrow [A(t)] \neq 0$.

$$[A_r] = \frac{1}{T}\sum_{j=0}^{N-1}\int_0^T \begin{bmatrix} a_{xx,j}(t) & a_{xy,j}(t) \\ a_{yx,j}(t) & a_{yy,j}(t) \end{bmatrix} e^{-ir\omega_T t} dt. \tag{15}$$

By introducing a change of variable, $\phi_j(t) = \Omega(t + jT)$, the pitch angle of the cutter $\phi_p(t) = \Omega T$, and considering that the directional matrix elements are non-zero only within the immersion interval $\langle\phi_{st}, \phi_{ex}\rangle$

$$\begin{aligned} [A_r] &= \frac{N}{2\pi}\int_{\phi_{st}}^{\phi_{ex}} \begin{bmatrix} a_{xx,j}(\phi) & a_{xy,j}(\phi) \\ a_{yx,j}(\phi) & a_{yy,j}(\phi) \end{bmatrix} e^{-ir\phi} d\phi \\ &= \frac{N}{2\pi}\begin{bmatrix} \alpha_{xx}^{(r)} & \alpha_{xy}^{(r)} \\ \alpha_{yx}^{(r)} & \alpha_{yy}^{(r)} \end{bmatrix}, \end{aligned} \tag{16}$$

where each term is dependent on the harmonic counter (r) as

$$\begin{aligned} \alpha_{xx}^{(r)} &= \frac{i}{2}[-c_0 K_r e^{-irN\phi} + c_1 e^{-ip_1\phi} - c_2 e^{ip_2\phi}]|_{\phi_{st}}^{\phi_{ex}}, \\ \alpha_{xy}^{(r)} &= \frac{1}{2}[-c_0 K_r e^{-irN\phi} + c_1 e^{-ip_1\phi} + c_2 e^{ip_2\phi}]|_{\phi_{st}}^{\phi_{ex}}, \\ \alpha_{yx}^{(r)} &= \frac{1}{2}[c_0 K_r e^{-irN\phi} + c_1 e^{-ip_1\phi} + c_2 e^{ip_2\phi}]|_{\phi_{st}}^{\phi_{ex}}, \\ \alpha_{yx}^{(r)} &= \frac{i}{2}[-c_0 K_r e^{-irN\phi} - c_1 e^{-ip_1\phi} + c_2 e^{ip_2\phi}]|_{\phi_{st}}^{\phi_{ex}}, \end{aligned}$$

where $p_1 = 2 + Nr$, $p_2 = 2 - Nr$, $c_0 = 2/(Nr)$, $c_1 = (K_r - i)/p_1$ and $c_2 = (K_r + i)/p_2$. The number of harmonics (r) of the tooth passing frequency (ω_T) to be considered for an accurate reconstruction of $[A(t)]$ depends on the immersion conditions and on the number of teeth in the cut. Altintas and Budak [8] and Budak and Altintas [9] proposed zero order and multi-frequency solutions, where the number of harmonics is $r = 0$ and $r \ge 1$, respectively. While the zero order solution is solved directly and analytically, and proven to be practical in most milling operations, the multi-frequency solution leads to improved accuracy when the radial immersion is small.

3.1. Zero order solution

In the most simplistic approximation, the average component of the *Fourier series* expansion is considered (i.e. $r = 0$) then

$$[A_0] = \frac{1}{T}\int_0^T [A(t)] dt = \frac{1}{\phi_p}\int_{\phi_{st}}^{\phi_{ex}} [A(\phi)] d\phi = \frac{N}{2\pi}\begin{bmatrix} \alpha_{xx} & \alpha_{xy} \\ \alpha_{yx} & \alpha_{yy} \end{bmatrix}, \tag{17}$$

where the integrated functions are given as

$$\begin{aligned} \alpha_{xx} &= \frac{1}{2}[\cos 2\phi - 2K_r\phi + K_r \sin 2\phi]_{\phi_{st}}^{\phi_{ex}}, \\ \alpha_{xy} &= \frac{1}{2}[-\sin 2\phi - 2\phi + K_r \cos 2\phi]_{\phi_{st}}^{\phi_{ex}}, \\ \alpha_{yx} &= \frac{1}{2}[-\sin 2\phi + 2\phi + K_r \cos 2\phi]_{\phi_{st}}^{\phi_{ex}}, \\ \alpha_{yy} &= \frac{1}{2}[-\cos 2\phi - 2K_r\phi - K_r \sin 2\phi]_{\phi_{st}}^{\phi_{ex}}. \end{aligned}$$

When the time dependant terms are neglected, the system loses its periodic variation, thus it becomes a time invariant system.

Then, the cutting force expression holds the following form at the critical stability border with vibration frequency ω_c

$$\{F(\omega)\} = \{P_0\}\delta(\omega - \omega_c) = \mathcal{F}(\{P_0\}\, e^{i\omega_c t}), \tag{18}$$

which is substituted into the dynamic force Eq. (13)

$$\{F(\omega)\} = \frac{1}{2} aK_t[A_0]\delta(\omega) * ((1 - e^{-i\omega T})[\Phi(\omega)]\{P_0\}\delta(\omega - \omega_c)),$$
$$\{P_0\}\delta(\omega - \omega_c) = \frac{1}{2} aK_t(1 - e^{-i\omega_c T})[A_0][\Phi(\omega_c)]\{P_0\}(\delta(\omega) * \delta(\omega - \omega_c)). \tag{19}$$

by applying the shifting theorem $\delta(\omega - a) * \delta(\omega - b) = \delta(\omega - (a + b))$

$$\{P_0\} = \frac{1}{2} aK_t(1 - e^{-i\omega_c T})[A_0][\Phi(\omega_c)]\{P_0\},$$

where $\omega_c T$ is the phase delay between the vibrations at successive tooth periods T. The average directional factors are now $[A_0]$ time independent, but dependent on the radial cutting constant (K_r) and the cutter immersion boundaries (ϕ_{st}, ϕ_{ex}). The stability of the dynamic milling is reduced to the following simple eigenvalue problem, which leads to a second order characteristic equation with coefficients dependant on the directional coefficients and the transfer functions:

$$det([I] + \Lambda[A_0][\Phi(\omega_c)]) = 0 \rightarrow \Lambda = -\frac{N}{4\pi} aK_t(1 - e^{-i\omega_c T}),$$
$$a_0\Lambda^2 + a_1\Lambda + 1 = 0 \rightarrow \Lambda = \Lambda_R + i\Lambda_I. \tag{20}$$

Finally, the critical axial depth of cut (a_{lim}) and spindle speeds (n [rpm]) are analytically calculated as

$$\left.\begin{aligned} a_{lim} &= -\frac{2\pi\Lambda_R}{NK_t}(1 + \kappa^2), \leftarrow \kappa = \frac{\Lambda_I}{\Lambda_R} \\ T &= \frac{1}{\omega_c}[(2k + 1)\pi) - 2\tan^{-1}\kappa], \rightarrow n = \frac{60}{NT} \end{aligned}\right\}. \tag{21}$$

The details of the derivations and the procedure to construct stability lobes can be found in [8]. The zero order solution has been applied to the stability of variable pitch cutters [14], ball end mills [15] and three-dimensional regenerative milling [16]. Altintas et al. [15] explained that the zero order solution is sufficient in most cases, because most of the vibration energy remains in the vicinity of modal frequencies, and the harmonics are low pass filtered by the structural modes.

3.2. Multi-frequency solution of chatter stability in milling

When the radial immersion of the cut is small, the milling process will exhibit highly intermittent directional factors which will lead to force waveforms with high frequency content. In such cases, the average directional factor $[A_0]$ may not be sufficient to predict the stability lobes at high spindle speeds with small radial immersions.

Due to the periodicity of the directional matrix ($[A(t)]$) the *Floquet theory* states that the periodic force has the following solution at the stability border where the tool vibrates with an additional vibration frequency ω_c

$$\{F(t)\} = e^{i\omega_c}\{P(t)\}, \qquad \{P(t)\} = \sum_{r=-\infty}^{\infty}\{P_r\}\, e^{ir\omega_T t}, \tag{22}$$

where $\{P(t)\}$ is periodic at tooth passing frequency ω_T. The force has the form according to the modulation theorem

$$\{F(\omega)\} = \sum_{r=-\infty}^{\infty}\{P_r\}\delta(\omega - (\omega_c + r\omega_T)). \tag{23}$$

Substituting (23) into (13):

$$\{F(\omega)\} = \frac{1}{2} aK_t[A(\omega)] * \left((1 - e^{-i\omega T})[\Phi(\omega)]\sum_{r=-\infty}^{\infty}\{P_r\}\delta(\omega - (\omega_c + r\omega_T))\right). \tag{24}$$

From the definition of *Dirac delta* function, the dynamic cutting force in frequency domain becomes

$$\{F(\omega)\} = \frac{1}{2} aK_t[A(\omega)] * \left(\sum_{r=-\infty}^{\infty}(1 - e^{-i(\omega_c + r\omega_T)T})[\Phi(\omega_c + r\omega_T)]\{P_r\}\delta(\omega - (\omega_c + r\omega_T))\right).$$

Since $r\,\omega_T T = r2\pi$ the delay term becomes independent on r

$$\{F(\omega)\} = \frac{1}{2} aK_t(1 - e^{-i\omega_c T})[A(\omega)] * \left(\sum_{r=-\infty}^{\infty}[\Phi(\omega_c + r\omega_T)]\{P_r\}\delta(\omega - (\omega_c + r\omega_T))\right). \tag{25}$$

The frequency domain solution can be used to include higher order harmonics at the expense of computational complexity as follows [17]:

$$[A(\omega)] = \cdots + \begin{bmatrix} \alpha_{xx}^{(-1)} & \alpha_{xy}^{(-1)} \\ \alpha_{yx}^{(-1)} & \alpha_{yy}^{(-1)} \end{bmatrix}\delta(\omega + \omega_T) + \begin{bmatrix} \alpha_{xx}^{(0)} & \alpha_{xy}^{(0)} \\ \alpha_{yx}^{(0)} & \alpha_{yy}^{(0)} \end{bmatrix}\delta(\omega) + \begin{bmatrix} \alpha_{xx}^{(+1)} & \alpha_{xy}^{(+1)} \\ \alpha_{yx}^{(+1)} & \alpha_{yy}^{(+1)} \end{bmatrix}\delta(\omega - \omega_T) + \cdots. \tag{26}$$

The directional matrix $[A(t)]$ is a periodic function at tooth passing frequency ω_T, and by substituting it into the dynamic cutting force (25)

$$\{F(\omega)\} = \frac{1}{2} aK_t(1 - e^{-i\omega_c T})\left(\sum_{r=-\infty}^{\infty}[A_r]\delta(\omega - r\omega_T)\right) * \left(\sum_{l=-\infty}^{\infty}[\Phi(\omega_c + l\omega_T)]\{P_l\}\delta(\omega - (\omega_c + l\omega_T))\right). \tag{27}$$

According to the *Cauchy product*

$$\{F(\omega)\} = \frac{1}{2} aK_t(1 - e^{-i\omega_c T}) \sum_{r=-\infty}^{\infty}\left(\left(\sum_{l=-\infty}^{\infty}[A_{r-l}][\Phi(\omega_c + l\omega_T)]\{P_l\} \times (\delta(\omega - (r - l)\omega_T) * \delta(\omega - (\omega_c + l\omega_T))\right)\right) \tag{28}$$

and the *shifting theorem*, the dynamic force becomes

$$\{F(\omega)\} = \sum_{r=-\infty}^{\infty}\left(\frac{1}{2} aK_t(1 - e^{-i\omega_c T})\left(\sum_{l=-\infty}^{\infty}[A_{r-l}][\Phi(\omega_c + l\omega_T)]\{P_l\}\right) \times \delta(\omega - (\omega_c + r\omega_T))\right).$$

Fourier coefficients of the force can be expressed from (23)

$$\{P_r\} = \frac{1}{2} aK_t(1 - e^{-i\omega_c T})\left(\sum_{l=-\infty}^{\infty}[A_{r-l}][\Phi(\omega_c + l\omega_T)]\{P_l\}\right), \tag{29}$$

where r is an integer number and varies between minus and plus infinity. By collecting the terms $\{P\}$, the stability of the system is defined by the following eigenvalue problem:

$$det([I] - \Lambda[G(\omega_c, \omega_T)]) = 0, \tag{30}$$

where the eigenvalue (Λ), eigenvector $\{P\}$ and oriented frequency response functions $[G(\omega_c,\omega_T)]$ with periodic directional factors $[A_{r-l}]$ are

$$\Lambda = \frac{1}{2}aK_t(1-e^{-i\omega_c T}),\qquad \{P\} = \begin{bmatrix}\{P_0\}\\ \{P_{-1}\}\\ \{P_1\}\\ \vdots\end{bmatrix},\qquad [G(\omega_c,\omega_T)] = \begin{bmatrix}[A_0][\Phi(\omega_c)] & [A_1][\Phi(\omega_c-\omega_T)] & [A_{-1}][\Phi(\omega_c+\omega_T)] & \cdots\\ [A_{-1}][\Phi(\omega_c)] & [A_0][\Phi(\omega_c-\omega_T)] & [A_{-2}][\Phi(\omega_c+\omega_T)] & \cdots\\ [A_1][\Phi(\omega_c)] & [A_2][\Phi(\omega_c-\omega_T)] & [A_0][\Phi(\omega_c+\omega_T)] & \cdots\\ \vdots & \vdots & \vdots & \ddots\end{bmatrix}. \quad (31)$$

If we take r number of tooth passing frequency harmonics into account, the dimension of the eigenvalue matrix becomes $M = n_{dof}(2r+1)$ where n_{dof} is the number of orthogonal flexibility directions considered in chatter. For example, if $r = 1$, and flexibility in (x, y) directions are considered ($n_{dof} = 2$), the matrix dimension becomes $M = 6$. The number of eigenvalues obtained from the solution would be equal to the size of the matrix (M). By noting that $e^{-i\omega_c T} = \cos\omega_c T - i\sin\omega_c T$, the eigenvalue number q can be represented by

$$\begin{aligned}\Lambda_q &= \Lambda_{R,q} + i\Lambda_{I,q} = \frac{1}{2}aK_t(1-e^{-i\omega_c T})\\ &= \frac{1}{2}aK_t[1-\cos\omega_c T + i\sin\omega_c T],\\ a &= \frac{[\Lambda_{R,q}(1-\cos\omega_c T)+\Lambda_{I,q}\sin\omega_c T]}{K_t(1-\cos\omega_c T)}\\ &\quad + i\frac{[\Lambda_{I,q}(1-\cos\omega_c T)-\Lambda_{R,q}\sin\omega_c T]}{K_t(1-\cos\omega_c T)}.\end{aligned} \quad (32)$$

Since the depth of a cut is a physical quantity, the imaginary part of the depth of the cut (a) must be zero, which leads to the following

$$\begin{aligned}&\Lambda_{I,q}(1-\cos\omega_c T) = \Lambda_{R,q}\sin\omega_c T \to \frac{\Lambda_{I,q}}{\Lambda_{R,q}} = \frac{\sin\omega_c T}{1-\cos\omega_c T},\\ &\omega_c T = \varepsilon + 2k\pi,\qquad \varepsilon = \pi - 2\psi,\qquad \psi = \tan^{-1}\frac{\Lambda_{I,q}}{\Lambda_{R,q}},\\ &a_q = \frac{[\Lambda_{R,q}(1-\cos\omega_c T)+\Lambda_{I,q}\sin\omega_c T]}{K_t(1-\cos\omega_c T)}.\end{aligned} \quad (33)$$

The spindle speed can be found as

$$\begin{aligned}&n = \frac{60}{NT} = \frac{60\omega_c}{N(\varepsilon+2k_l\pi)},\quad k_l = 1,2,\ldots,\\ &a_q = \frac{\Lambda_{R,q}}{K_t}\left[1+\left(\frac{\Lambda_{I,q}}{\Lambda_{R,q}}\right)^2\right].\end{aligned} \quad (34)$$

However, the evaluation of the phase shift (ε) between the waves requires the solution of eigenvalues Λ_q, which is dependent on the evaluation of frequency response functions ($\Phi(\omega_c \pm l\omega_T)$) at the harmonics of tooth passing frequencies. Hence, unlike in the zero order solution, there is no direct solution to the depth of the cut. Instead, a range of spindle speeds must be scanned for each chatter frequency in order to find the eigenvalues. For a given speed, the eigenvalues and the corresponding value of depth of cut are evaluated using (32). The computational load is significantly higher in the multi-frequency solution in comparison to the zero frequency solution. There will be M number of eigenvalues, and at each iteration the most conservative and positive depth of cut must be considered as a final solution. However, the zero order solution, which considers only the average of directional factors $[A_0]$, gives the stability lobes directly within few seconds.

4. Semi-discrete time domain solution

Insperger and Stépán [10] presented an analytical solution of chatter stability in a discrete time domain. The periodic milling dynamics with time varying, self-excitation and delay terms expressed in (10) are organized as first order equations as

$$(\dot{q}(t)) = [L(t)](q(t)) + [R(t)]\{q(t-T)\}, \quad (35)$$

where

$$[L(t)] = \begin{bmatrix}[0] & [I]\\ \delta[M]^{-1}[A(t)] - [\omega_n^2] & -[2\zeta\omega_n]\end{bmatrix},$$

$$[R(t)] = \begin{bmatrix}[0] & [0]\\ -\delta[M]^{-1}(A(t)) & [0]\end{bmatrix},\qquad \{q(t)\} = \begin{Bmatrix}x(t)\\ y(t)\\ \dot{x}(t)\\ \dot{y}(t)\end{Bmatrix},$$

$$[A(t)] = \begin{bmatrix}a_{xx}(t) & a_{xy}(t)\\ a_{yx}(t) & a_{yy}(t)\end{bmatrix},\qquad \delta = \frac{1}{2}aK_t,\qquad [M]^{-1} = \begin{bmatrix}\frac{\omega_{nx}^2}{k_x} & 0\\ 0 & \frac{\omega_{ny}^2}{k_y}\end{bmatrix},$$

$$[2\zeta\omega_n] = \begin{bmatrix}2\varsigma_x\omega_{nx} & 0\\ 0 & 2\varsigma_y\omega_{ny}\end{bmatrix},\qquad [\omega_n^2] = \begin{bmatrix}\omega_{nx}^2 & 0\\ 0 & \omega_{ny}^2\end{bmatrix}. \quad [J1]$$

The delay period T is divided into m number of discrete time intervals Δt, i.e. $T = m\,\Delta t$, as shown in Fig. 2. Let the value of $\{q(t_i)\}$ at the current time t_i simply be expressed as $\{q_i\}$ and at time $t_i - T$ as $\{q(t_i - T)\} = \{q[(i-m)\Delta t]\} = \{q_{i-m}\}$. When the sampling interval Δt is considerably smaller, the value of $\{q(t_i - T)\}$ can be approximated by averaging the values at two consecutive sampling intervals as

$$\begin{aligned}\{q(t-T)\} &\approx \left\{q\left(t_i + \frac{\Delta t}{2} - T\right)\right\}\\ &\approx \frac{\{q(t_i - T + \Delta t)\} + \{q(t_i - T)\}}{2}\\ &= \frac{\{q_{i-m+1}\} + \{q_{i-m}\}}{2} \to t \in [t_i, t_{i+1})\end{aligned} \quad (36)$$

The dynamics of the system represented in (35) is re-written at discrete time intervals as

$$\{\dot{q}_i(t)\} = [L_i]\{q_i(t)\} + \frac{1}{2}[R_i](\{q_{i-m+1}\} + \{q_{i-m}\}) \quad (37)$$

The differential equation $\{\dot{q}(t)\}$ has homogenous $\{q_{Hi}(t)\}$ and particular $\{q_{Pi}(t)\}$ solutions at the small time interval Δt as

$$\{q_i(t)\} = \{q_{Hi}(t)\} + \{q_{Pi}(t)\}. \quad (38)$$

The homogeneous solution is obtained as

$$\{\dot{q}_{Hi}(t)\} = [L_i]\{q_{Hi}(t)\} \to \{q_{Hi}(t)\} = e^{[L_i](t-t_i)}\{C_0\}, \quad (39)$$

where $\{C_0\}$ depends on the initial conditions. The particular solution is given by

$$\begin{aligned}&\{\dot{q}_{Pi}(t)\} = [L_i]\{q_{Pi}(t)\} + \frac{1}{2}[R_i](\{q_{i-m+1}\} + \{q_{i-m}\}),\\ &\{q_{Pi}(t)\} = e^{[L_i](t-t_i)}\{u(t)\} = -\frac{1}{2}[L_i]^{-1}[R_i](\{q_{i-m+1}\} + \{q_{i-m}\}).\end{aligned} \quad (40)$$

The complete solution of the system is

$$\begin{aligned}\{q_i(t)\} &= \{q_{Hi}(t)\} + \{q_{Pi}(t)\}\\ &= e^{[L_i](t-t_i)}\{C_0\} - \frac{1}{2}[L_i]^{-1}[R_i](\{q_{i-m+1}\} + \{q_{i-m}\})\end{aligned} \quad (41)$$

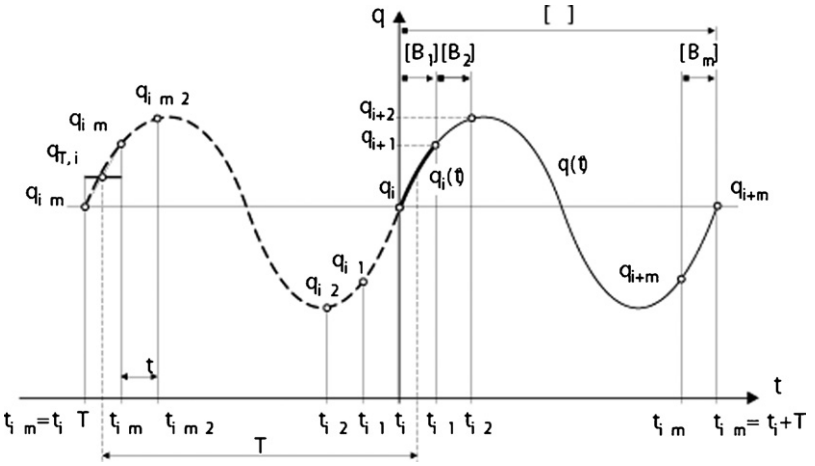

Fig. 2. Discretization of a periodic signal.

when the system is at $t = t_i$.

$$\{q_i\} = \{C_0\} - \frac{1}{2}[L_i]^{-1}[R_i](\{q_{i-m+1}\} + \{q_{i-m}\}) \to \{C_0\} = \{q_i\} + \frac{1}{2}[L_i]^{-1}[R_i](\{q_{i-m+1}\} + \{q_{i-m}\}). \quad (42)$$

Since the solution is valid at discrete time intervals $\Delta t = t_{i+1} - t_i$, the states at time $t = t_{i+1}$ are

$$\{q_{i+1}\} = e^{[L_i]\Delta t}\{q_i\} + \frac{1}{2}(e^{[L_i]\Delta t} - [I])[L_i]^{-1}[R_i](\{q_{i-m+1}\} + \{q_{i-m}\}). \quad (43)$$

The solution requires the previous value $\{q_i\}$ and values a delay before ($\{q_{i-m}\}$,$\{q_{i-m+1}\}$). The series of equations are expressed at discrete time intervals:

$$\{z_{i+1}\} = [B_i]\{z_i\}, \quad (44)$$

where

$$\{z_i\} = \begin{Bmatrix} \{q_i\} \\ \{q_{i-1}\} \\ \{q_{i-2}\} \\ \vdots \\ \{q_{i-m+1}\} \\ \{q_{i-m}\} \end{Bmatrix}_{2(m+1)\times 1}, \quad [B_i] = \begin{bmatrix} e^{[L_i]\Delta t} & [0] & \cdots & [0] & \frac{1}{2}(e^{[L_i]\Delta t} - [I])[L_i]^{-1} & \frac{1}{2}(e^{[L_i]\Delta t} - [I])[L_i]^{-1}[R_i] \\ [I] & [0] & \cdots & [0] & [0] & [0] \\ [0] & [I] & \cdots & [0] & [0] & [0] \\ \vdots & \vdots & \ddots & \vdots & \vdots & \vdots \\ [0] & [0] & \cdots & [I] & [0] & [0] \\ [0] & [0] & \cdots & [0] & [I] & [0] \end{bmatrix}_{2(m+1)\times 2(m+1)}.$$

Note that the directional matrix $[A(t)]$ varies at each sampling time interval, as do the state matrixes $[L(t)]$ and $[R(t)]$ which are dependent on $[A(t)]$The time varying milling process can be simulated by solving the discrete set of recursive Eq. (43) at Δt time intervals. Since the process is periodic at tooth passing interval T, it is sufficient to solve the equations at m number of time intervals.

The stability of the system can be evaluated by expressing (44) at m number of intervals within the tooth period T

$$\{z_{i+m}\} = [\Phi]\{z_i\} = [B_m]\cdots[B_2][B_1]\{z_i\}. \quad (45)$$

According to *Floquet theory*, the linear periodic system (35) will be unstable if any of the eigenvalues of the transition matrix $[\Phi]$ have a modulus greater than one, critically stable if the modulus is unity and stable if the moduluses of all the eigenvalues are less than unity. The zero order frequency domain solution directly provides the critical stability borders, the lobes; in contrast, the semi-discrete time domain solution must be searched by scanning a range of trial spindle speeds and depths of cuts. The semi-discrete time domain solution considers the time varying, periodic coefficients $[A(t)]$ described at discrete time intervals Δt; hence the accuracy of the stability is expected to be higher, especially when the process is highly interrupted at small radial cutting depths.

5. Simulations

The proposed stability solutions are validated through numerical simulations and extensive experimentation [14–16,18]. A sample simulation and experimental results for a cutter with two circular inserts are shown in Fig. 3. The process was half immersion down milling with strong periodic excitation. The time domain simulation results are obtained from a numerical simulation of the physical process which includes exact cutter geometry, time varying dynamic forces, and exact chip geometry which considers the saturation and other nonlinearities in the milling process [19]. The numerical algorithm predicts the history of chip thickness, vibrations, feed-vibration and run out marks on the finish surface. The details of the structural dynamic parameters and cutting conditions can be found in [18]. It can be seen from Fig. 3 that the zero order solution matches with the numerical solution perfectly, and took only few seconds to compute. The experimental results also indicate that the stability is predicted accurately; i.e. the process is unstable at 9500 rpm with a 4.5 mm depth of cut, but stable at the same depth when the speed is increased to 14,000 rpm.

When the cutting process is highly intermittent at high spindle speeds, i.e. low radial immersion and small number of teeth, the zero order solution cannot predict the lobes as accurately as the

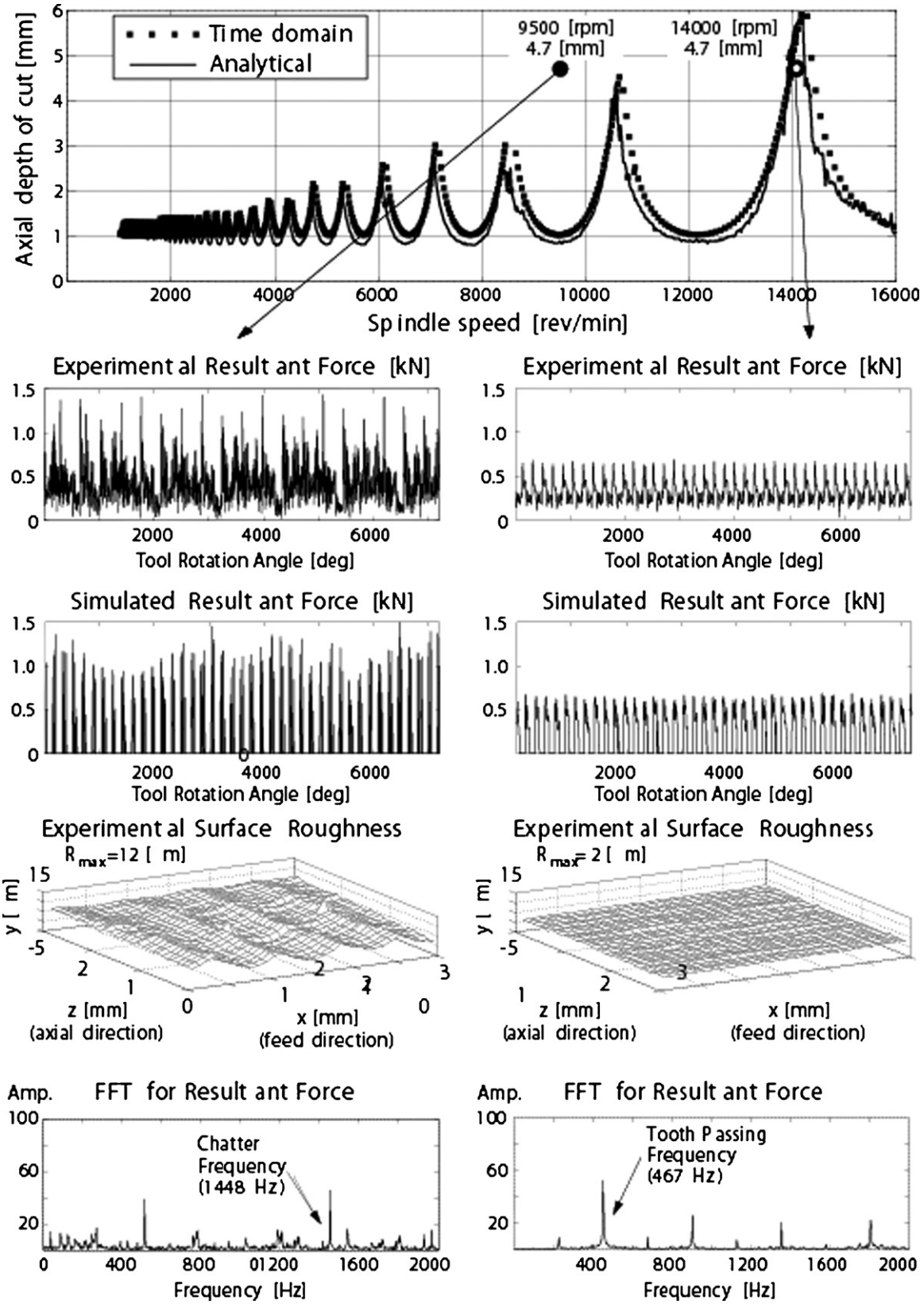

Fig. 3. Comparison of the zero order solution against numerical and experimental results. Cutter: Bull nosed cutter with two inserts. Cutting conditions: Half immersion down milling, feed rate 0.050 mm/tooth. See Ref. [18] for the cutting coefficients and structural dynamic parameters.

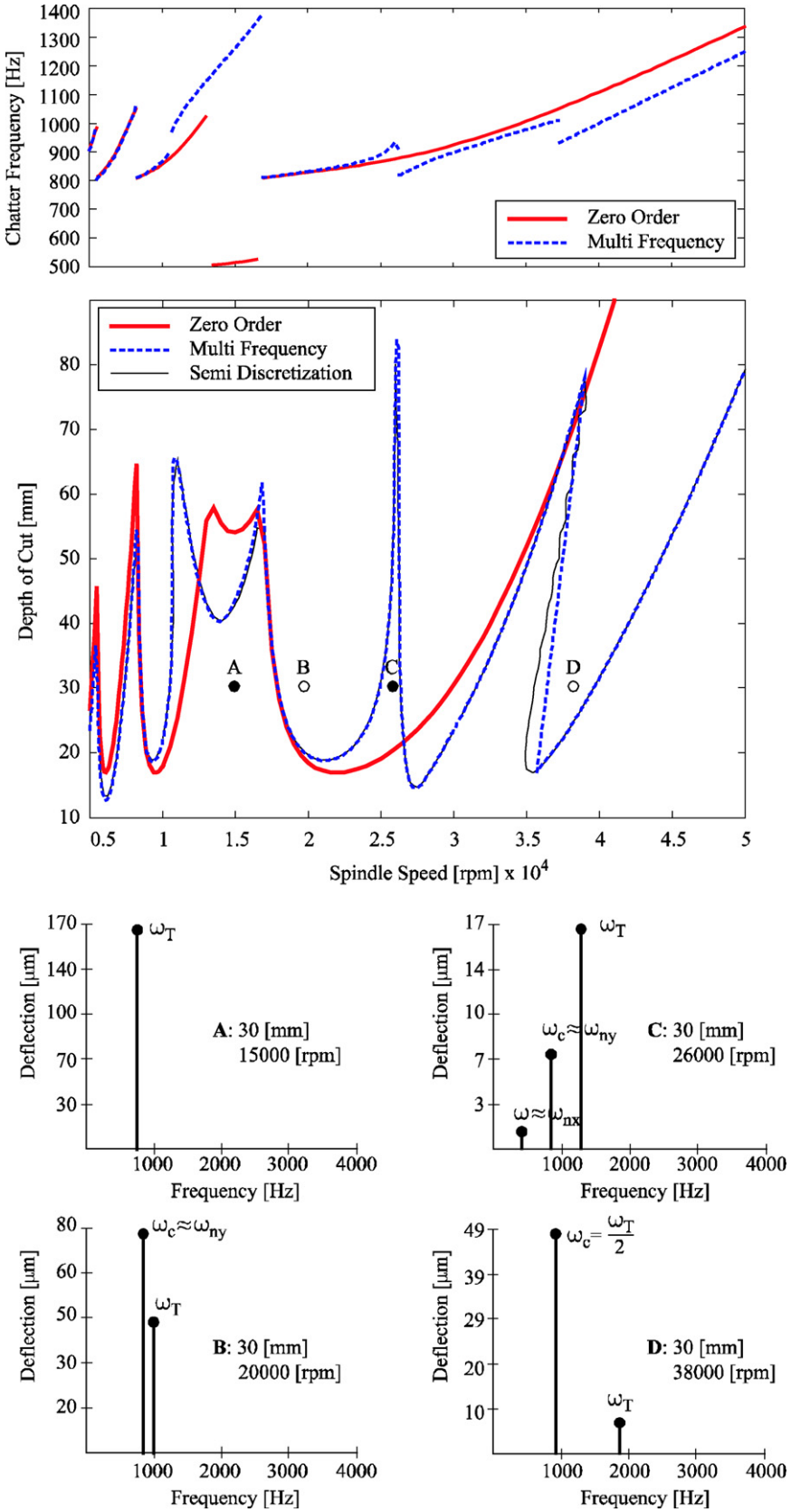

Fig. 4. Comparison of the zero order, multi-frequency solution with $r = 3$ harmonics, and semi-discretization-based solutions. Cutter: three flutes with zero helix. Cutting condition: Half immersion down milling. Cutting coefficients: $K_t = 900\ \mathrm{N/nm^2}$, $K_r = 270\ \mathrm{N/nm^2}$. Structural dynamic parameters: $\omega_{nx} = 510$ Hz, $\omega_{ny} = 802$ Hz; $\zeta_x = 0.04$, $\zeta_y = 0.05$; $k_x = 96.2 \times 10^{-6}$ N/m, $k_y = 47.5 \times 10^{-6}$ N/m.

multi-frequency and semi-discrete solutions which consider the time varying directional factors. The problem will be most evident at lobes which start from the lobe where the tooth passing and natural frequency of the structure matches. A specific example is created to illustrate the problem as shown in Fig. 4. The cutter has three flutes with a zero helix, cutting aluminum with half immersion down milling mode. The structural modes are at 510 Hz and 802 Hz, which corresponds to the highest stability pockets around 10,200 rpm and 16,040 rpm, respectively. The process is highly intermittent due to a low immersion and small number of teeth. The simulations took about 25 min for multi-frequency solution, and 49 min by the semi-discretization method, respectively. The computer was Pentium with two 2.4 GHz CPU. It can be seen that the zero order, multi-frequency and semi-discretization methods give almost the same stability lobes until the stability pocket zone around 10,200 rpm, but deviate afterwards where the zero order solution cannot capture the influence of time varying directional factors on the stability. The process is stable at point A where forced vibrations occur at the tooth passing frequency ω_T = 750 Hz. The process chatters around the natural mode of 802 Hz at point B. However, after 16,040 rpm, zero order solution cannot predict the added lobes which occur at 26,000 rpm and 35,000 rpm. However, both multi-frequency [17] and semi-discrete [11] solutions predict the added lobes in perfect agreement. The multi-frequency solution used three harmonics of the directional factors, and the semi-discrete solution used a frequency scale of 40 times the highest natural frequency (i.e. 40 Hz × 802 Hz). The physics of added lobes are explained by Merdol and Altintas in [17], and briefly discussed here. The higher harmonics of directional factors flip the frequency response function $G(\omega_c - l\omega_T)$ from left to right, bringing it to the zone of modal frequency on the right $G(\omega_c)$. This creates additional stability lobes. This phenomenon is illustrated at cutting condition C. For example, at a = 30 mm depth of cut and n = 26,000 rpm, the process is stable. The tooth passing frequency is ω_T = 1300 Hz, which is considered as G[802–1300 Hz] = $G(-498$ Hz) and G[510–1300 Hz] = $G(-790$ Hz) by the multi-frequency solution. Both results flip the frequency response functions and bring them to the zones of 510 Hz and 802 Hz, creating a stability pocket at 26,000 rpm. At spindle speed 38,000 rpm (point D), the process chatters exactly at the half of the tooth passing frequency. However, as the depth of the cut increases from 30 mm towards 60 mm, the added stability lobe appears due to the same phenomenon. Readers must be cautioned, however, that this phenomenon rarely occurs in practice, since the machine is usually not operated at tooth passing frequencies beyond the natural modes. Operated at a higher mode, the machine would always distort the added lobes. If there is no higher mode, the machine can operate at very high speeds without unbalance issues.

6. Conclusion

The chatter stability is dependent on the cutting force coefficients, structural dynamic parameters of the machine tool and work-piece, and cutting conditions. The milling process has time periodic dynamics which differ from time-invariant single point cutting operations. This paper presents the two most commonly used frequency and discrete time domain stability solutions for milling operations.

The frequency domain solution is proposed by Altintas and Budak [8] and Budak and Altintas [9]. When the average of periodic directional factors are used, the stability solution is reduced to direct evaluation of spindle speed and depth of cut; hence the stability lobes are calculated directly in a few seconds without any iterative search. This is called the zero order solution, and can be used in machining practice where the immersion is larger than a quarter of the cutter diameter, and tooth passing frequencies are not beyond the natural modes of the structure.

When the process is highly intermittent, which occurs at low radial immersions and a small number of teeth, the time variation of the dynamic process needs to be considered. This is especially true at tooth passing frequencies beyond the natural modes. Instead of taking only the average value, higher harmonics of directional factors need to be considered in the frequency domain, or multi-frequency, solution of Altintas and co-workers [9,17]. The frequency domain solution can use raw FRF measurements directly, without having to identify modal parameters. It also predicts the stability borders directly.

The semi-discretization method of Insperger and Stépán [10,11] considers the time variation of directional factors at each discrete sampling interval; hence, it can predict the stability lobes at any speed. The accuracy of the semi-discretization method is limited only by its sampling interval. The computation time depends on the number of modes in the system and sampling interval. Complex cutter-part engagements, state dependent delays such as variable pitch and spindle speed variations can be handled. While both multi-frequency and semi-discretization methods predict the milling chatter stability accurately, both require an iterative search of critically stable lobe borders; therefore, they are computationally more time consuming.

The stability of milling is currently well understood and predicted at high speeds by the frequency and time domain solutions as presented in the article. The stability theories are well established and can handle any cutting process dynamics provided that the physical models are sound and correct. However, it is still challenging to model the dynamic cutting process at low speeds where the spindle rotates at lobes higher than 10. The clearance face of the tool rubs against the wavy surface finish which adds unknown process damping to the process, and increases the stable depth of cuts [20]. The modelling of process damping physics is still a research challenge, but once modelled current stability laws can be used to predict the chatter stability lobes at low speeds as well.

References

[1] Koenigsberger, F., Tlusty, J., 1967, Machine Tool Structures-Vol. I: Stability Against Chatter, Pergamon Press.
[2] Tobias, S.A., 1965, Machine Tool Vibration, Blackie and Sons Ltd..
[3] Tlusty, J., 1986, Dynamics of High Speed Milling, Transactions of ASME Journal of Engineering for Industry, 108:59–67.
[4] Tlusty, J., Ismail, F., 1981, Basic Nonlinearity in Machining Chatter, Annals of the CIRP, 30:21–25.
[5] Smith, S., Tlusty, J., 1993, Efficient Simulation Programs for Chatter in Milling, CIRP Annals, 42/1: 463–466.
[6] Sridhar, R., Hohn, R.E., Long, G.W., 1968, A Stability Algorithm for the General Milling Process, Transactions of ASME Journal of Engineering for Industry, 90:330–334.
[7] Minis, I., Yanushevsky, T., Tembo, R., Hocken, R., 1990, Analysis of Linear and Nonlinear Chatter in Milling, Annals of the CIRP, 39:459–462.
[8] Altintas, Y., Budak, E., 1995, Analytical Prediction of Stability Lobes in Milling, Annals of the CIRP, 44/1: 357–362.
[9] Budak, E., Altintas, Y., 1998, Analytical Prediction of Chatter Stability Conditions for Multi-degree of Systems in Milling. Part I. Modelling, Part II. Applications, Transactions of ASME Journal of Dynamic Systems Measurement and Control, 120:22–30.
[10] Insperger, T., Stépán, G., 2000, Stability of the Milling Process, Periodica Polytechnica, 44:47–57.
[11] Insperger, T., Stépán, G., 2004, Updated Semi-discretization Method for Periodic Delay-Differentilal Equations with Discrete Delay, International Journal for Numerical Methods in Engineering, 61:117–141.
[12] Govekar, E., Gradisek, J., Kalveram, M., Insperger, T., Weinert, K., Stépán, G., Grabec, I., 2005, On Stability and Dynamics of Milling at Small Radial Immersion, CIRP Annals Manufacturing Technology, 54:357–362.
[13] Bayly, P.V., Halley, J.E., Mann, B.P., Davies, M.A., 2003, Stability of Interrupted Cutting by Temporal Finite Element Analysis, Transactions of ASME Journal of Manufacturing Science and Engineering, 125:220–225.

[14] Altintas, Y., Engin, S., Budak, E., 1999, Analytical Prediction of Chatter Stability and Design for Variable Pitch Cutters, Transactions of ASME Manufacturing and Engineering and Science, 121:173–178.
[15] Altintas, Y., Shamoto, E., Lee, P., Budak, E., 1999, Analytical Prediction of Stability Lobes in Ball End Milling, Transactions of ASME Journal of Manufacturing Science and Engineering, 121:586–592.
[16] Altintas, Y., 2001, Analytical Prediction of Three Dimensional Chatter Stability in Milling, Japan Society of Mechanical Engineers International, 44/3: 717–723.
[17] Merdol, D., Altintas, Y., 2004, Multi Frequency Solution of Chatter Stability for Low Immersion Milling, Transactions of ASME Journal of Manufacturing Science and Engineering, 126/3: 459–466.
[18] Altintas, Y., Engin, S., 2001, Generalized Modeling of Mechanics and Dynamics of Milling Cutters, CIRP Annals, 50/1: 25–30.
[19] CUTPRO Milling, Advanced Milling Process Simulation Software, Manufacturing Automation Laboratories Inc. (www.malinc.com).
[20] Altintas, Y., Weck, M., 2004, Chatter Stability in Metal Cutting and Grinding, Annals of the CIRP, 53/2: 619–642. (Key Note Paper of STC-M).